Thermochimica Acta 497 (2010) 101–108

Contents lists available at ScienceDirect

Thermochimica Acta

journal homepage: www.elsevier.com/locate/tca

Synthesis and thermal behavior of Janus dendrimers, part 1☆

Tero Tuuttila, Manu Lahtinen, Noora Kuuloja, Juhani Huuskonen, Kari Rissanen*

Nanoscience Center, Department of Chemistry, University of Jyväskylä, P.O. Box 35, FIN-40014, Jyväskylä, Finland

ARTICLE INFO

Article history:
Received 12 November 2008
Received in revised form 25 August 2009
Accepted 26 August 2009
Available online 3 September 2009

Keywords:
Polyester dendrimers
Thermal properties
TGA
DSC

ABSTRACT

Eight Janus-type dendrimers up to the second generation were synthesized, and their thermal properties were evaluated. Compounds consist of the dendritic bisMPA based polyester moieties, and either 3,4-dihexyloxybenzoic acid or 3,4-dihexadecyloxybenzoic acid moieties, attached to opposite sides of the pentaerythritol core. The structures of the molecules were verified with ^{1}H NMR, ^{13}C NMR, ESI TOF mass spectrometry and elemental analysis. The thermal stability was evaluated by thermogravimetric analysis, displaying onset decomposition temperatures (T_d) ranging from 241 to 308 °C. Phase transitions were studied by differential scanning calorimetry. Based on the performed studies it was confirmed that OH terminated dendrimers **2**, **4**, **6** and **8** exhibited liquid crystalline phases. Also, the X-ray powder diffraction measurements were accomplished for the dendrimers having terminal hydroxyl groups.

1. Introduction

Dendrimers are highly branched macromolecules having well-defined structures, which consist of a multivalent core, layers of AB_x branching monomers (generations), and defined number of terminal groups [1–3]. Two common stepwise synthetic approaches have been utilized to build up dendrimers in order to control the shape, size, functionality, and, as a result, properties of the dendrimers. In the divergent method [4–6] compounds are constructed generation by generation from the core to the periphery. In the convergent manner [7,8] dendrimers are constructed from the periphery to the core, by preparing initially dendrons of appropriate size, which are attached to the core. Due to the versatile properties of dendrimers, arising from the structural features, they are potential candidates for various applications such as drug delivery systems [9,10], light harvesting [11–13], and catalysis [14–17].

Janus dendrimers, also called bow-tie or block co-dendrimers, characterized by the diverse peripheral groups on opposite sides, are relatively new class of dendrimers [18–27]. The interest towards the dendritic Janus molecules stem from their bisfunctional character, applicable in various purposes. Recent studies on Janus dendrimers have, for example, demonstrated self-assembling properties [21,28–30] as well as potential use in medical applications [31,32].

Peripheral groups are primarily responsible for the thermal properties of the dendrimers. It was first reported by Fréchet and co-workers [33] that alteration of the polarity of the terminal groups has an influence on glass transition temperatures. Since then, several groups have reported the influence of the end group functionality [34–36] as well as other structural modifications [37,38] on the thermal properties of the dendritic molecules. Percec et al. have extensively studied the self-assembling dendritic molecules that exhibit thermotropic liquid-crystal phases [39–44].

Herein we report the synthesis of small amphiphilic Janus dendrimers up to the second generation. Our interest was to study the thermal behavior of Janus dendrimers having opposite terminal groups of significantly different polarity. These dendrimers, emanating from the pentaerythritol core, consist of bisMPA based polyester branches, having either acetonide groups or hydroxyl groups in the periphery, and opposite 3,4-dialkyloxybenzoic acids containing alkyl chain ends of different length (C_6 or C_{16}).

2. Experimental

2.1. Materials and instrumentations

All the starting materials were purchased from major suppliers and used without any further purification. Dichloromethane (DCM) was dried over 4 Å sieves. The pentaerythritol based core molecule, $(OH)_2$-PE-[G1]-acetonide, was synthesized according to published procedure [27]. Isopropylidene-2,2-bis(hydroxymethyl)propionic acid anhydride was prepared according to procedure described by Malkoch et al. [45]. 3,4-Dihexyloxybenzoic acid and 3,4-dihexadecyloxybenzoic acid was prepared by using a modified literature procedure [46]. Column chromatography was performed with Merck 60 F254 silica gel, particle size 0.040–0.063 mm. ^{1}H and ^{13}C NMR spectra were recorded on a Bruker Avance DRX 500

☆ Janus dendrimers are C_6 and C_{16} alkyl chain based polyester dendrimers.

* Corresponding author. Fax: +358 14 260 2501.
E-mail address: kari.t.rissanen@jyu.fi (K. Rissanen).

0040-6031/$ – see front matter © 2009 Elsevier B.V. All rights reserved.
doi:10.1016/j.tca.2009.08.018

NMR (500.13 and 125.76 MHz) spectrometer in $CDCl_3$ or DMSO-*d6* solution. The solvent signal was used as an internal standard. Mass spectral data was obtained with Micromass LCT Electronspray ionization time-of-flight (ESI TOF) instrument with either positive-ion or negative-ion mode. Thermal behavior of the compounds was determined on power compensation type PerkinElmer PYRIS DIAMOND DSC. The measurements were carried out under nitrogen atmosphere (flow rate 50 mL min^{-1}) using 50 μL sealed aluminum sample pans. The sealing was made by using a 30 μL aluminum pan with capillary holes to ascertain good thermal contact between a sample and pan, and to minimize free volume inside the pan. The temperature calibration was made using two standard materials (n-decane, In) and energy calibration by an indium standard (28.45 J g^{-1}). Typically, following temperature profile was used for each sample: a sample was heated from −40 to desired end temperature (from 120 to 200 °C) with a heating rate of 10 °C/min, followed by 1 min hold at the end temperature, and cooled down to −40 °C with a rate of 10 °C/min. The sample was held at −40 °C for 5 min and heated for a second time, respectively. Sample weights of 3–6 mg were used on the measurements. Finally, the sample weight was checked afterwards to monitor weight losses that may have occurred during the scans. The uncertainty for measured temperatures was less than 0.8 °C for all measurements. The thermal decomposition was examined with PerkinElmer TGA7 thermogravimetric analyzer. Measurements were carried out in platinum pans under synthetic air atmosphere (flow rate of 50 mL/min) with heating rate of 10 °C/min on temperature range of 25–700 °C. To improve determination of decomposition onset by removing solvent/moisture residues from the samples, an isothermal step at 150 °C for 3 h was introduced to the heating profile. The temperature calibration of instrument was carried out using Curie-point calibration technique (Alumel, Ni, Perkalloy, Fe). The weight balance was calibrated by measuring the standard weight of 50 mg at room temperature. The sample weights used in the measurements were about 5–9 mg. The decomposition onset was obtained using step tangent method at which 5% decomposition is occurred (taken account the initial weight loss occurred at isothermal step). The X-ray powder diffraction data was measured with PANalytical X'Pert PRO diffractometer in Bragg–Brentano geometry using Johansson monochromator (α_1 setup) to produce pure CuKα_1 radiation (1.5406 Å; 45 kV, 30 mA) and step-scan technique in 2θ range of 3–70°. The data was collected by X'Celerator detector in continuous scanning mode with a step size of 0.017 and using sample dependently counting times of 100 s per step. Programmable divergence slit (PDS) was used in automatic mode to set irradiated length on sample to 15 mm together with 15 mm incident beam mask. Soller slits of 0.02° rad were used on both incident and diffracted beam sides together with anti-scatter 4° and 13 mm, respectively. Before further analyses, the diffraction data were converted from automatic slit mode (ADS) to a fixed slit mode (FDS) data by the tools implemented in Highscore Plus v. 2.2c software package. Hand-ground powder samples were prepared on a silicon-made zero-background holder using petrolatum jelly as an adhesive. Preliminary studies with polarizing optical microscope (POM) were accomplished to confirm the presence of mesomorphic phases. More detailed characterization of the mesomorphic phases will be presented elsewhere.

2.2. Synthesis

2.2.1. 3,4-Hexyloxybenzoic acid

4.64 g (97%) of white solid. ^{1}H NMR ($CDCl_3$, 500 MHz): δ_{ppm} = 0.88–0.93 (m, 6H, C*H*$_3$), 1.33–1.35 (m, 8H, (C*H*$_2$)$_2$CH$_3$), 1.41–1.50 (m, 4H, O(CH$_2$)$_2$C*H*$_2$), 1.76–1.89 (m, 4H, OCH$_2$C*H*$_2$), 3.99–4.06 (m, OC*H*$_2$), 6.84 (d, 1H, Ar*H* position 5, *J* = 8.5 Hz), 7.56 (d, 1H, Ar*H* position 2, *J* = 1.9 Hz), 7.67 (dd, 1H, Ar*H* position 6, *J* = 8.5, 1.9 Hz). ^{13}C NMR ($CDCl_3$, 126 MHz): δ_{ppm} = 13.97 (*C*H$_3$), 22.57 (*C*H$_2$CH$_3$), 25.64 and 25.78 (*C*H$_2$CH$_2$CH$_2$OAr), 29.05 and 29.15 (*C*H$_2$CH$_2$OAr), 31.55 and 31.58 (*C*H$_2$CH$_2$CH$_3$), 69.01 and 69.23 (*C*H$_2$OAr), 111.89 (Ar*C* position 5), 114.59 (Ar*C* position 2), 122.37 (Ar*C* position 1), 124.24 (Ar*C* position 6), 148.49 (Ar*C* position 3), 153.57 (Ar*C* position 4), 171.67 (*C*O). ESI TOF MS: *m*/*z* calcd. for $C_{19}H_{30}O_4$ 312.21 $[M-H]^-$, found 312.19 $[M-H]^-$.

2.2.2. 3,4-Hexadecyloxybenzoic acid

4.49 g (92%) of white solid. ^{1}H NMR ($CDCl_3$, 500 MHz): δ_{ppm} = 0.88 (t, 6H, C*H*$_3$, J = 7.0 Hz), 1.26–1.36 (m, 48H, (C*H*$_2$)$_{12}$CH$_3$), 1.45–1.51 (m, 4H, OCH$_2$CH$_2$C*H*$_2$), 1.80–1.87 (m, 4H, OCH$_2$C*H*$_2$), 4.03–4.07 (m, 4H, OC*H*$_2$), 6.89 (d, 1H, Ar*H* position 5, *J* = 8.5 Hz), 7.58 (d, 1H, Ar*H* position 2, *J* = 2.0 Hz), 7.71 (dd, 1H, Ar*H* position 6, *J* = 8.5, 2.0 Hz). ^{13}C NMR ($CDCl_3$, 126 MHz): δ_{ppm} = 14.10 (alkyl *C*H$_3$), 22.69 (*C*H$_2$CH$_3$), 25.97 and 26.02 (*C*H$_2$CH$_2$CH$_2$OAr), 29.07 and 29.19 (*C*H$_2$CH$_2$OAr), 29.36–29.71 ((*C*H$_2$)$_{10}$CH$_2$CH$_2$CH$_3$), 31.93 (*C*H$_2$CH$_2$CH$_3$), 69.09 and 69.34 (*C*H$_2$OAr), 111.99 (Ar*C* position 5), 114.72 (Ar*C* position 2), 121.27 (Ar*C* position 1), 124.44 (Ar*C* position 6), 148.63 (Ar*C* position 3), 153.95 (Ar*C* position 4), 170.12 (*C*O). ESI TOF MS: *m*/*z* calcd. for $C_{39}H_{70}O_4$ 601.52 $[M-H]^-$, found 601.50 $[M-H]^-$.

2.2.3. 3,4-Bis-hexyloxybenzoic ester-PE-[G1]-acetonide (**1**)

(OH)$_2$-PE-[G1]-acetonide (1.50 g, 3.34 mmol), 3,4-hexyloxybenzoic acid (2.37 g, 7.36 mmol) and DPTS (0.98 g, 3.34 mmol) were dissolved in dry CH_2Cl_2 (60 mL) and dry THF (15 mL). The mixture was flushed with nitrogen (30 min), and DCC (1.38 g, 6.69 mmol) added in the flask. The mixture was stirred at room temperature for 48 h under nitrogen atmosphere. DCC-urea was filtered off and washed with small amount of CH_2Cl_2. Solvent was evaporated, and the crude product was purified by column chromatography (SiO_2) eluting with hexane/ethyl acetate (4:1) to give 1.97 g (56%) of viscous oil. ^{1}H NMR ($CDCl_3$, 500 MHz): δ_{ppm} = 0.90 (t, 6H, C*H*$_3$, *J* = 7.0 Hz), 0.91 (t, 6H, C*H*$_3$, *J* = 7.0 Hz), 1.13 (s, 6H, bisMPA-C*H*$_3$), 1.31 (s, 6H, acetonide-C*H*$_3$), 1.33–1.36 (m, 16H, (C*H*$_2$)$_2$CH$_3$), 1.40 (s, 6H, acetonide-C*H*$_3$), 1.45–1.51 (m, 8H, C*H*$_2$CH$_2$CH$_2$OAr), 1.79–1.86 (m, 8H, C*H*$_2$CH$_2$OAr), 3.62 (d, 4H, bisMPA-C*H*$_2$, *J* = 11.9 Hz), 4.02 (t, 4H, C*H*$_2$OAr, *J* = 6.6 Hz), 4.04 (t, 4H, C*H*$_2$OAr, *J* = 6.6 Hz), 4.17 (d, 4H, bisMPA-C*H*$_2$, *J* = 11.9 Hz), 4.40 (s, 4H, PE-C*H*$_2$), 4.48 (s, 4H, PE-C*H*$_2$), 6.83 (d, 2H, Ar*H* position 5, *J* = 8.5 Hz), 7.49 (d, 2H, Ar*H* position 2, *J* = 2.0 Hz), 7.58 (dd, 2H, Ar*H* position 6, *J* = 8.5 Hz, *J* = 2.0 Hz). ^{13}C NMR ($CDCl_3$, 126 MHz): δ_{ppm} = 13.94 and 13.96 (alkyl *C*H$_3$), 18.41 (bisMPA-*C*H$_3$), 21.77 (acetonide-*C*H$_3$), 22.54 and 22.56 (*C*H$_2$CH$_3$), 25.36 (acetonide-*C*H$_3$), 25.60 and 25.64 (*C*H$_2$CH$_2$CH$_2$OAr), 28.99 and 29.13 (*C*H$_2$CH$_2$OAr), 31.51 and 31.55 (*C*H$_2$CH$_2$CH$_3$), 42.25 (*C*-bisMPA), 43.31 (PE-*C*), 62.50 and 62.52 (PE-*C*H$_2$), 66.03 (bisMPA-*C*H$_2$), 69.02 and 69.30 (*C*H$_2$OAr), 98.15 (acetonide-*C*), 112.00 (Ar*C* position 5), 114.34 (Ar*C* position 2), 121.61 (Ar*C* position 1), 123.63 (Ar*C* position 6), 148.70 (Ar*C* position 3), 153.57 (Ar*C* position 4), 165.75 (*C*O), 173.66 (*C*O). ESI TOF MS: *m*/*z* calcd. for $C_{59}H_{92}O_{16}$ 1079.63 $[M+Na]^+$, found 1079.57 $[M+Na]^+$. Anal. Calcd for $C_{59}H_{92}O_{16}$: C 67.02%, H 8.77%. Found: C 66.85%, H 8.83%.

2.2.4. 3,4-Bis-hexyloxybenzoic ester-PE-[G1]-(OH)$_4$ (**2**)

1 (1.75 g, 1.65 mmol) was dissolved in CH_2Cl_2 (15 mL) and diluted with MeOH (15 mL). 2 teaspoons of Dowex 50W resin was added, and the mixture stirred at 50 °C for 19 h. Resin was filtered off, and washed with small amount of CH_2Cl_2. Filtrate was concentrated to give 1.55 g (96%) of white solid. ^{1}H NMR ($CDCl_3$, 500 MHz): δ_{ppm} = 0.90 (t, 6H, C*H*$_3$, *J* = 7.0 Hz), 0.90 (t, 6H, C*H*$_3$, *J* = 7.0 Hz), 1.08 (s, 6H, bisMPA-C*H*$_3$), 1.33–1.35 (m, 16H, (C*H*$_2$)$_2$CH$_3$), 1.46–1.51 (m, 8H, C*H*$_2$CH$_2$CH$_2$OAr), 1.78–1.86 (m, 8H, C*H*$_2$CH$_2$OAr), 3.13 (s, 4H, O*H*), 3.74 (d, 4H, bisMPA-C*H*$_2$, *J* = 11.3 Hz), 3.86 (d, 4H, bisMPA-C*H*$_2$, *J* = 11.3 Hz), 4.01 (t, 4H, C*H*$_2$OAr, *J* = 6.5 Hz), 4.03 (t, 4H, C*H*$_2$OAr,

J = 6.5 Hz), 4.36 (s, 4H, PE-CH_2), 4.50 (s, 4H, PE-CH_2), 6.83 (d, 2H, ArH position 5, J = 8.5 Hz), 7.49 (d, 2H, ArH position 2, J = 2.0 Hz), 7.59 (dd, 2H, ArH position 6, J = 8.5 Hz, J = 2.0 Hz). ^{13}C NMR ($CDCl_3$, 63 MHz): δ_{ppm} = 13.95 and 13.96 (alkyl CH_3), 17.15 (bisMPA-CH_3), 22.55 and 22.56 (CH_2CH_3), 25.61 and 25.66 ($CH_2CH_2CH_2OAr$), 28.99 and 29.14 (CH_2CH_2OAr), 31.51 and 31.55 ($CH_2CH_2CH_3$), 43.55 (PE-C), 49.92 (C-bisMPA), 61.77 and 62.06 (CH_2-PE), 68.01 (bisMPA-CH_2), 69.05 and 69.37 (CH_2OAr), 111.99 (ArC position 5), 114.44 (ArC position 2), 121.37 (ArC position 1), 123.75 (ArC position 6), 148.74 (ArC position 3), 153.79 (ArC position 4), 166.00 (CO), 175.15 (CO). ESI TOF MS: m/z calcd. for $C_{53}H_{84}O_{16}$ 999.57 $[M+Na]^+$, found 999.53 $[M+Na]^+$. Anal. Calcd for $C_{53}H_{84}O_{16}$: C, 65.14%, H 8.66%. Found: C 65.19%, H, 8.69%.

2.2.5. 3,4-Bis-hexyloxybenzoic ester-PE-[G2]-acetonide (**3**)

2 (0.93 g, 0.95 mmol), anhydride of bisMPA (1.63 g, 4.92 mmol) and DMAP (69 mg, 0.75 mmol) were dissolved in pyridine (1.5 mL) and CH_2Cl_2 (6 mL) and stirred at room temperature for 68 h. 1 mL of water was added with vigorous stirring for 2 h to quench the anhydride. The mixture was then diluted with 100 mL of CH_2Cl_2, and washed with 10% $NaHSO_4$ (3 × 50 mL), 10% Na_2CO_3 (3 × 50 mL), and with brine (50 mL). Organic layer was dried over anhydrous $MgSO_4$ and solvent evaporated. The product was further purified by column chromatography (SiO_2) eluting with hexane/ethyl acetate (3:2) to give 1.16 g (76%) of glassy solid. ^{1}H NMR ($CDCl_3$, 500 MHz): δ_{ppm} = 0.90 (t, 6H, CH_3, J = 7.0 Hz), 0.91 (t, 6H, CH_3, J = 7.0 Hz), 1.09 (s, 12H, G2-CH_3), 1.28 (s, 6H, G1-CH_3), 1.32 (s, 12H, acetonide-CH_3), 1.33–1.38 (overlapped peaks, 28H, $(CH_2)_2CH_3$ + acetonide-CH_3), 1.45–1.51 (m, 8H, CH_2CH$_2$CH$_2$OAr), 1.79–1.86 (m, 8H, CH_2CH$_2$OAr), 3.56 (dd, 8H, G2-CH_2, J = 11.9 Hz, J = 2.1 Hz), 4.01 (t, 4H, CH_2OAr, J = 6.6 Hz), 4.03 (t, 4H, CH_2OAr, J = 6.6 Hz), 4.11 (d, 8H, G2-CH_2, J = 11.8 Hz), 4.33 (ABq, 8H, G1-CH_2, J = 11.1 Hz), 4.34 (s, 4H, PE-CH_2), 4.45 (s, 4H, PE-CH_2), 6.83 (d, 2H, ArH position 5, J = 8.5 Hz), 7.48 (d, 2H, ArH position 2, J = 2.0 Hz), 7.56 (dd, 2H, ArH position 6, J = 8.5 Hz, J = 2.0 Hz). ^{13}C NMR ($CDCl_3$, 63 MHz): δ_{ppm} = 13.96 and 13.98 (alkyl CH_3), 17.65 (G1-CH_3), 18.45 (G2-CH_3), 22.02 (acetonide-CH_3), 22.55 and 22.57 (CH_2CH_3), 25.11 (acetonide-CH_3), 25.62 and 25.67 ($CH_2CH_2CH_2OAr$), 29.01 and 29.16 (CH_2CH_2OAr), 31.52 and 31.57 ($CH_2CH_2CH_3$), 42.03 (G2-C), 43.11 (PE-C), 47.07 (G1-C), 62.21 and 63.04 (PE-CH_2), 64.86 (G1-CH_2), 65.90 and 65.94 (G2-CH_2), 69.05 and 69.32 (CH_2OAr), 98.07 (acetonide-C), 111.99 (ArC position 5), 114.36 (ArC position 2), 121.49 (ArC position 1), 123.59 (ArC position 6), 148.75 (ArC position 3), 153.65 (ArC position 4), 165.59 (CO), 172.01 (G1-CO), 173.44 (G2-CO). ESI TOF MS: m/z calcd. for $C_{85}H_{132}O_{28}$ 1623.88 $[M+Na]^+$, found 1624.02 $[M+Na]^+$. Anal. Calcd for $C_{85}H_{132}O_{28}$: C 63.73%, H 8.31%. Found: C 63.73%, H 8.17%.

2.2.6. 3,4-Bis-hexyloxybenzoic ester-PE-[G2]-$(OH)_8$ (**4**)

The procedure is the same as the synthesis of **2**. Compound **3** (0.99 g, 0.62 mmol) and 2 teaspoons of Dowex 50W were used to give 0.89 g (98%) of white solid. ^{1}H NMR ($CDCl_3$, 500 MHz): δ_{ppm} = 0.90 (t, 6H, CH_3, J = 7.0 Hz), 0.91 (t, 6H, CH_3, J = 7.0 Hz), 1.04 (s, 12H, G2-CH_3), 1.28 (s, 6H, G1-CH_3), 1.33–1.36 (m, 16H, $(CH_2)_2CH_3$), 1.44–1.50 (m, 8H, CH_2CH$_2$CH$_2$OAr), 1.78–1.86 (m, 8H, CH_2CH$_2$OAr), 3.26 (s, 8H, OH), 3.67 (dd, 8H, bisMPA-CH_2, J = 11.3 Hz, J = 4.8 Hz), 3.77 (dd, 8H, bisMPA-CH_2, J = 11.2 Hz, J = 3.5 Hz), 4.00 (t, 4H, CH_2OAr, J = 6.6 Hz), 4.03 (t, 4H, CH_2OAr, J = 6.6 Hz), 4.34 (ABq, 8H, G1-CH_2, J = 11.1 Hz), 4.37 (s, 4H, PE-CH_2), 4.47 (s, 4H, PE-CH_2), 6.83 (d, 2H, ArH position 5, J = 8.5 Hz), 7.48 (d, 2H, ArH position 2, J = 2.0 Hz), 7.56 (dd, 2H, ArH position 6, J = 8.5 Hz, J = 2.0 Hz). ^{13}C NMR ($CDCl_3$, 63 MHz): δ_{ppm} = 13.94 and 13.96 (alkyl CH_3), 17.08 (G2-CH_3), 17.96 (G2-CH_3), 22.53 and 22.55 (CH_2CH_3), 25.60 and 25.65 ($CH_2CH_2CH_2OAr$), 28.99 and 29.14 (CH_2CH_2OAr), 31.50 and 31.54 ($CH_2CH_2CH_3$), 42.88 (PE-C), 46.83 (G1-C), 49.80 (G2-C), 62.60 and 63.62 (PE-CH_2), 64.85 (G1-CH_2), 67.22 and 67.34 (G2-CH_2), 69.05 and 69.38 (CH_2OAr), 111.99 (ArC position 5), 114.41 (ArC position 2), 121.23 (ArC position 1), 123.70 (ArC position 6), 148.74 (ArC position 3), 153.84 (ArC position 4), 165.94 (CO), 172.57 (G1-CO), 175.01 (G2-CO). ESI TOF MS: m/z calcd. for $C_{73}H_{116}O_{28}$ 1463.76 $[M+Na]^+$, found 1463.93 $[M+Na]^+$. Anal. Calcd for $C_{73}H_{116}O_{28}$: C 60.82%, H 8.12%. Found: C 60.73%, H 8.03%.

2.2.7. 3,4-Bis-hexadecyloxybenzoic ester-PE-[G1]-acetonide (**5**)

The procedure is the same as the synthesis of **1**. $(OH)_2$-PE-[G1]-acetonide (1.00 g, 2.23 mmol), 3,4-hexadecyloxybenzoic acid (2.96 g, 4.91 mmol), DPTS (0.66 g, 2.23 mmol), and DCC (1.20 g, 5.80 mmol) in CH_2Cl_2 (90 mL) was used to give 2.23 g (62%) of white solid. ^{1}H NMR ($CDCl_3$, 500 MHz): δ_{ppm} = 0.87 (t, 12H, CH_3, J = 7.0 Hz), 1.13 (s, 6H, bisMPA-CH_3), 1.26 (overlapped peaks, 96H, $(CH_2)_{12}CH_3$), 1.31 (s, 6H, acetonide-CH_3), 1.41 (s, 6H, acetonide-CH_3), 1.44–1.50 (m, 8H, CH_2CH$_2$CH$_2$OAr), 1.79–1.86 (m, 8H, CH_2CH$_2$OAr), 3.63 (d, 4H, bisMPA-CH_2, J = 11.9 Hz), 4.01 (t, 4H, CH_2OAr, J = 6.6 Hz), 4.03 (t, 4H, CH_2OAr, J = 6.6 Hz), 4.17 (d, 4H, bisMPA-CH_2, J = 11.9 Hz), 4.40 (s, 4H, PE-CH_2), 4.48 (s, 4H, PE-CH_2), 6.83 (d, 2H, ArH position 5, J = 8.5 Hz), 7.49 (d, 2H, ArH position 2, J = 2.0 Hz), 7.58 (dd, 2H, ArH position 6, J = 8.5 Hz, J = 2.0 Hz). ^{13}C NMR ($CDCl_3$, 126 MHz): δ_{ppm} = 14.08 (alkyl CH_3), 18.44 (bisMPA-CH_3), 21.80 (acetonide-CH_3), 22.67 (CH_2CH_3), 25.37 (acetonide-CH_3), 25.98 and 26.04 ($CH_2CH_2CH_2OAr$), 29.08 and 29.23 (CH_2CH_2OAr), 29.35–29.70 ($(CH_2)_{10}CH_2CH_2CH_3$), 31.92 ($CH_2CH_2CH_3$), 42.27 (C-bisMPA), 43.33 (PE-C), 62.53 (PE-CH_2), 66.05 (bisMPA-CH_2), 69.06 and 69.34 (CH_2OAr), 98.17 (acetonide-C), 112.02 (ArC position 5), 114.38 (ArC position 2), 121.63 (ArC position 1), 123.65 (ArC position 6), 148.73 (ArC position 3), 153.60 (ArC position 4), 165.77 (CO), 173.67 (CO). ESI TOF MS: m/z calcd. for $C_{99}H_{172}O_{16}$ 1641.26 $[M+Na]^+$, found 1641.14 $[M+Na]^+$. Anal. Calcd for $C_{99}H_{172}O_{16}$: C 73.47%, H 10.71%. Found: C 73.20%, H 10.64%.

2.2.8. 3,4-Bis-hexadecyloxybenzoic ester-PE-[G1]-$(OH)_4$ (**6**)

The procedure is the same as the synthesis of **2**. Compound **5** (2.03 g, 1.25 mmol) and teaspoons of Dowex 50W resin was used to give 1.86 g (97%) of white solid. ^{1}H NMR ($CDCl_3$, 500 MHz): δ_{ppm} = 0.86 (t, 12H, CH_3, J = 7.0 Hz), 1.08 (s, 6H, bisMPA-CH_3), 1.26 (overlapped peaks, 96H, $(CH_2)_{12}CH_3$), 1.44–1.50 (m, 8H, CH_2CH$_2$CH$_2$OAr), 1.79–1–86 (m, 8H, CH_2CH$_2$OAr), 3.07 (s, 4H, OH), 3.75 (d, 4H, bisMPA-CH_2, J = 11.3 Hz), 3.87 (d, 4H, bisMPA-CH_2, J = 11.3 Hz), 4.01 (t, 4H, CH_2OAr, J = 6.6 Hz), 4.03 (t, 4H, CH_2OAr, J = 6.6 Hz), 4.36 (s, 4H, PE-CH_2), 4.50 (s, 4H, PE-CH_2), 6.83 (d, 2H, ArH position 5, J = 8.5 Hz), 7.49 (d, 2H, ArH position 2, J = 2.0 Hz), 7.59 (dd, 2H, ArH position 6, J = 8.5 Hz, J = 2.0 Hz). ^{13}C NMR ($CDCl_3$, 126 MHz): δ_{ppm} = 14.08 (alkyl CH_3), 17.16 (bisMPA-CH_3), 22.67 (CH_2CH_3), 25.98 and 26.04 ($CH_2CH_2CH_2OAr$), 29.07 and 29.23 (CH_2CH_2OAr), 29.35–29.70 ($(CH_2)_{10}CH_2CH_2CH_3$), 31.92 ($CH_2CH_2CH_3$), 43.58 (PE-C), 49.91 (C-bisMPA), 61.76 and 62.04 (PE-CH_2), 68.13 (bisMPA-CH_2), 69.07 and 69.40 (CH_2OAr), 111.99 (ArC position 5), 114.46 (ArC position 2), 121.37 (ArC position 1), 123.75 (ArC position 6), 148.76 (ArC position 3), 153.81 (ArC position 4), 166.00 (CO), 175.16 (CO). ESI TOF MS: m/z calcd. for $C_{93}H_{164}O_{16}$ 1561.20 $[M+Na]^+$, found 1561.26 $[M+Na]^+$. Anal. Calcd for $C_{93}H_{164}O_{16}\cdot 1/2\ H_2O$: C 72.19%, H 10.75%. Found: C 72.29%. H 10.75%.

2.2.9. 3,4-Bis-hexadecyloxybenzoic ester-PE-[G2]-acetonide (**7**)

The procedure is the same as the synthesis of **3**. Compound **6** (1.23 g, 0.80 mmol), anhydride of bisMPA (1.38 g, 4.17 mmol), and DMAP (59 mg, 0.48 mmol) in pyridine (1.5 mL) and CH_2Cl_2 (6 mL) were used. Purified by column chromatography (SiO_2) eluting with hexane/ethyl acetate (2:1) to give 1.53 g (89%) of white solid. ^{1}H NMR ($CDCl_3$, 500 MHz): δ_{ppm} = 0.88 (t, 12H, CH_3, J = 7.0 Hz), 1.09 (s, 12H, G2-CH_3), 1.26 (overlapped peaks, 96H, $(CH_2)_{12}CH_3$)), 1.28 (s, 6H, G1-CH_3), 1.32 (s, 12H, acetonide-CH_3), 1.36 (s, 12H,

acetonide-CH_3), 1.43–1.50 (m, 8H, CH_2CH$_2$CH$_2$OAr), 1.78–1.86 (m, 8H, CH_2CH$_2$OAr), 3.56 (dd, 8H, G2-CH_2, J = 11.9 Hz, J = 2.1 Hz), 4.01 (t, 4H, CH_2OAr, J = 6.6 Hz), 4.03 (t, 4H, CH_2OAr, J = 6.6 Hz), 4.11 (d, 8H, G2-CH_2, J = 11.7 Hz), 4.34 (ABq, 8H, G1-CH_2, J = 11.2 Hz), 4.34 (s, 4H, PE-CH_2), 4.45 (s, 4H, PE-CH_2), 6.82 (d, 2H, ArH position 5, J = 8.5 Hz), 7.48 (d, 2H, ArH position 2, J = 2.0 Hz), 7.55 (dd, 2H, ArH position 6, J = 8.5 Hz, J = 2.0 Hz). ^{13}C NMR (CDCl$_3$, 63 MHz): δ_{ppm} = 14.08 (alkyl CH$_3$), 17.66 (G1-CH$_3$), 18.46 (G2-CH$_3$), 22.05 (acetonide-CH$_3$), 22.67 (CH$_2$CH$_3$), 25.10 (acetonide-CH$_3$), 26.00 and 26.07 (CH$_2$CH$_2$CH$_2$OAr), 29.10 and 29.26 (CH$_2$CH$_2$OAr), 29.34–29.72 ((CH$_2$)$_{10}$CH$_2$CH$_2$CH$_3$), 31.92 (CH$_2$CH$_2$CH$_3$), 42.03 (G2-C), 43.12 (PE-C), 47.08 (G1-C), 62.29 and 63.05 (PE-CH$_2$), 64.87 (G1-CH$_2$), 65.91 and 65.95 (G2-CH$_2$), 69.07 and 69.36 (CH$_2$OAr), 98.07 (acetonide-C), 112.00 (ArC position 5), 114.40 (ArC position 2), 121.51 (ArC position 1), 123.59 (ArC position 6), 148.78 (ArC position 3), 153.67 (ArC position 4), 165.59 (CO), 172.01 (G1-CO), 173.43 (G2-CO). ESI TOF MS: m/z calcd. for $C_{125}H_{212}O_{28}$ 2158.51 [M+Na]$^+$, found 2185.71 [M+Na]$^+$. Anal. Calcd for $C_{125}H_{212}O_{28}$: C 69.41%, H 9.88%. Found: C 69.65%, H 9.90%.

2.2.10. 3,4-Bis-hexadecyloxybenzoic ester-PE-[G2]-(OH)$_8$ (**8**)

The procedure is the same as the synthesis of **2**. **7** (1.13 g, 0.52 mmol) and 2 teaspoons of Dowex 50W were used to give 0.76 g (73%) of white solid. ^{1}H NMR (CDCl$_3$, 500 MHz): δ_{ppm} = 0.88 (t, 12H, CH_3, J = 7.0 Hz), 1.04 (s, 12H, G2-CH_3) (overlapped peaks, 96H, (CH_2)$_{12}$CH$_3$)), 1.29 (s, 6H, G1-CH_3), 1.44.1.50 (m, 8H, CH_2CH$_2$CH$_2$OAr), 1.78–1.85 (m, 8H, CH_2CH$_2$OAr), 3.13 (s, 8H, OH), 3.68 (dd, 8H, bisMPA-CH_2, J = 11.3 Hz, J = 4.8 Hz), 3.80 (dd, 8H, bisMPA-CH_2, J = 11.2 Hz, J = 3.5 Hz), 4.00 (t, 4H, CH_2OAr, J = 6.6 Hz), 4.03 (t, 4H, CH_2OAr, J = 6.6 Hz), 4.35 (ABq, 8H, G1-CH_2, J = 11.1 Hz), 4.37 (s, 4H, PE-CH_2), 4.47 (s, 4H, PE-CH_2), 6.83 (d, 2H, ArH position 5, J = 8.5 Hz), 7.48 (d, 2H, ArH position 2, J = 2.0 Hz), 7.56 (dd, 2H, ArH position 6, J = 8.5 Hz, J = 2.0 Hz). ^{13}C NMR (CDCl$_3$, 126 MHz): δ_{ppm} = 14.09 (alkyl CH$_3$), 17.11 (G2-CH$_3$), 22.68 (CH$_2$CH$_3$), 26.00 and 26.07 (CH$_2$CH$_2$CH$_2$OAr), 29.09 and 29.26 (CH$_2$CH$_2$OAr), 29.36–29.71 ((CH$_2$)$_{10}$CH$_2$CH$_2$CH$_3$), 31.92 (CH$_2$CH$_2$CH$_3$), 42.88 (PE-C), 46.89 (G1-C), 49.78 (G2-C), 62.66 and 63.72 (PE-CH$_2$), 64.93 (G1-CH$_2$), 67.65 and 67.78 (G2-CH$_2$), 69.09 and 69.45 (CH$_2$OAr), 112.00 (ArC position 5), 114.46 (ArC position 2), 121.26 (ArC position 1), 123.72 (ArC position 6), 148.79 (ArC position 3), 153.88 (ArC position 4), 165.97 (CO), 172.59 (G1-CO), 175.06 (G2-CO). ESI TOF MS: m/z calcd. for $C_{113}H_{196}O_{28}$ 2025.38 [M+Na]$^+$, found 2025.45 [M+Na]$^+$. Anal. Calcd for $C_{113}H_{196}O_{28}$·3/2 H_2O: C 66.87%, H 9.88%. Found: C 66.90, H 9.76.

3. Results and discussion

3.1. Synthesis

The prepared first generation (G1) Janus dendrimers are shown in Scheme 1. Dendrimers were built around pentaerythritol (PE) by attaching initially the first layer of dendritic polyester moieties on the other side, and then 3,4-dialkylbenzoic acid moieties on the opposite side of the pentaerythritol.

The preparation of the half protected first generation dendritic core, (OH)$_2$-PE-[G1]-acetonide, has been described previously by our group [27]. Monodendrons, 3,4-dihexyloxybenzoic acid and 3,4-dihexadecyloxybenzoic acid, were obtained from etherification of methyl 3,4-dihydroxybenzoate with corresponding n-alkyl bromide in DMF, followed by the hydrolysis of ester group with KOH in refluxing EtOH/THF solution [46]. Monodendrons were attached to the dendritic core using DCC esterification in the presence of 4-(dimethylamino)pyridinium p-toluenesulfonate (DPTS) [47] as a catalyst, giving compounds **1** and **5** in 51 and 62% yields, respectively, after chromatographic purification. Deprotection of the isopropylidene groups of the compounds **1** and **5** were done by

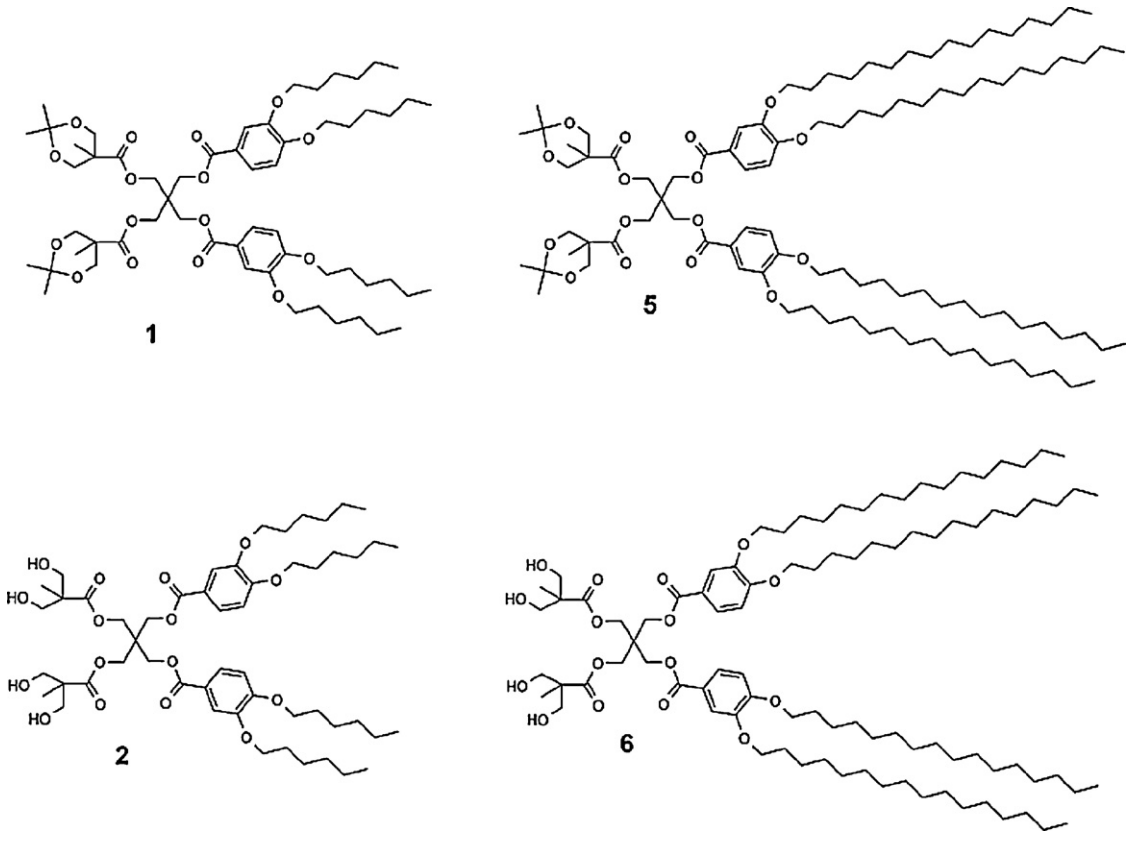

Scheme 1. The first generation Janus dendrimers.

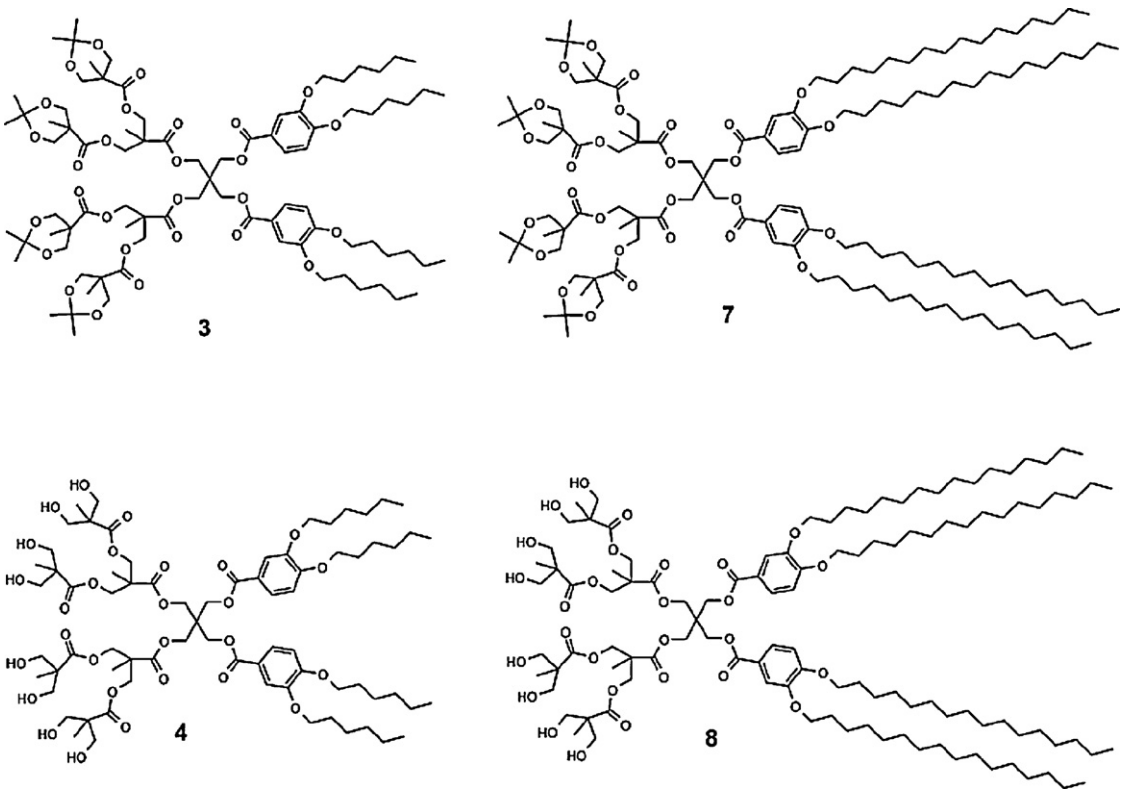

Scheme 2. The second generation Janus dendrimers.

DOWEX 50W resin in the DCM/MeOH solution at 50 °C. Compounds were stirred with the resin until deprotection was complete. The resin was filtered, and the filtrate concentrated to give the first generation hydroxyl terminated dendrimers **2** and **6** in 96 and 97% yields, respectively.

The second generation (G2) dendrimers (Scheme 2) were prepared by divergent method utilizing the anhydride coupling. Hydroxyl terminated dendrimers **2** and **6** were allowed to react with isopropylidene-2,2-bis(methoxy)propionic anhydride [45] in DCM in the presence of 4-dimethylaminopyridine (DMAP) and pyridine. The crude product was dissolved in DCM followed by extraction with 10% $NaHSO_4$, 10% Na_2CO_3 and brine. Finally, purification by column chromatography gave compounds **3** and **7** in 76 and 89% yields, respectively. The preparation of the hydroxyl terminated second generation dendrimers were performed in the presence of DOWEX resin as described above, giving compounds **4** and **8** in 98 and 73% yields, respectively. Hydroxyl terminated compounds **2**, **4**, **6**, and **8** were further recrystallized from the solution of ethyl acetate and hexane.

3.2. Thermogravimetric studies

Thermogravimetric analysis (TGA) was utilized to evaluate the thermal stability of the dendrimers. The onset decomposition temperatures (T_d) were recorded at a heating rate of 10 °C/min. An isothermal step at 150 °C for 3 h was included to the heating profile, to remove the traces of solvent/water. Mass losses on the isothermal step ranged from 0.2 to 1.7%. Since the decomposition of the dendrimers started relatively slowly, step tangent method at 5-wt% mass loss was utilized, in order to avoid overestimating the thermal stability. TGA curves are shown in Fig. 1, and decomposition temperatures collected in Table 1.

The T_d-values of C_6 alkylated dendrimers ranged from 268 to 308 °C, indicating fairly high thermal stability, and compounds were completely decomposed at around 600 °C. The T_d-values of C_6 dendrimers slightly increased with increasing molecular weight by additional generation. In addition, hydroxyl terminated dendrimers displayed higher T_d-values than corresponding acetonide protected dendrimers, probably on account of hydrogen bonding interactions. These results correlate with the previously reported results of thermal behavior of bisMPA based polyester dendrimers [37]. On the other hand, all the T_d-values of C_{16} dendrimers were around 250 °C, showing little or no effect of the size or the terminal groups of the polyester moieties on thermal stability of the dendrimers. The higher T_d-values of the C_6 alkylated dendrimers are most likely caused by more dense packing of the dendrimers with shorter alkyl chains, allowing stronger bonding interactions (hydrogen bonding and weak π–π-interactions) of the dendritic moieties. Packing in the case of C_{16} alkylated dendrimers is probably more disordered due to the entanglement of the alkyl chains.

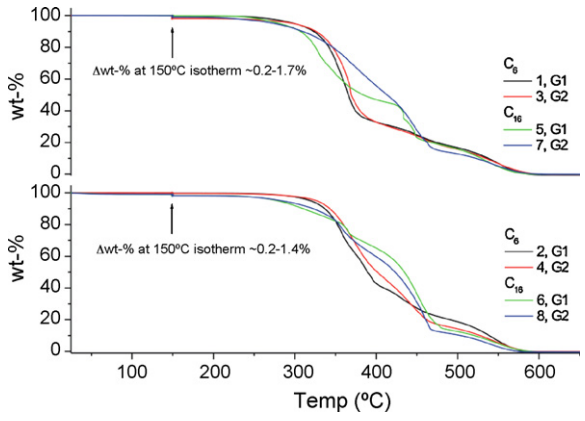

Fig. 1. TG curves of acetonide protected dendrimers **1**, **3**, **5**, and **7** (upper), and hydroxyl terminated dendrimers **2**, **4**, **6**, and **8** (lower).

Table 1
Thermal properties of compounds **1**–**8**.

Compound	Mw	Thermal transitions (°C) and their corresponding enthalpy and/or heat capacity changes (kJ mol^{-1}) [kJ mol^{-1} °C^{-1}][a]		DSC range of scan (°C)	TGA decomposition temperature (°C)[b]
		Heating scans	Cooling scans		
1	1057.38	1st: g −17.8 [0.40] i 2nd: g −17.6 [0.38] i	1st: –	−40 to 160	268 (0.25)[c]
5	1618.47	1st: k 52.0 (135.61) i 2nd: k 50.8 (107.58) i	1st: i 44.9 (−105.82) k	−40 to 120	250 (0.22)
2	977.25	1st: k 71.7 (60.64) i 2nd: g 7.6 [0.28] LC 33.7 (0.81) i	1st: i 31.4 (−0.79) LC 7.4 [0.13] g	−40 to 160	295 (0.26)
6	1538.33	1st: k 65.6 (128.52) LC 114.1 (2.26) i 2nd: k 62.9 (82.11) LC 114.3 (2.37) i	1st: i 113.1 (−2.43) LC 53.5 (−78.80) k	−40 to 140	254 (0.71)
3	1601.98	1st: k 38.1 (52.61) i 2nd: g −8.6 [0.60] i	1st: –	−40 to 150	289 (1.74)
7	2163.07	1st: k 44.5 (131.59) i 2nd: k 43.3 (106.31) i	1st: i 36.7 (−110.99) k	−40 to 150	241 (0.85)
4	1441.72	1st: k {72.9 (26.90), 104.9 (−3.71)}[d] 115.0 (54.78) i 2nd: g 26.3 [0.51], 46.8 (−30.15) k 109.7 (56.32) i	1st: i 62.5 (−4.63) LC 22.5 [0.20] g	−40 to 200	308 (0.30)
8	2002.81	1st: k {67.9 (103.01), 71.3 (−7.93), 73.4 (25.91)}[e] 110.3 (62.81) LC 140.6 (1.06) i 2nd: k {67.4 (75.28), 73.0 (−68.32)}[f] 111.0 (57.21) LC 140.4 (1.15) i 3rd: k {67.6 (75.20), 74.2 (−43.62)}[f] 110.1 (57.00) LC 140.2 (1.07) i	1st: i 139.8 (−1.17) LC 62.3 (−71.43) k 2nd: i 139.6 (−1.18) LC 62.3 (−79.92) k	−40 to 200	253 (1.37)

Abbreviations: k, crystalline; i, isotropic liquid; g, glass; LC, liquid-crystal phase. Crystallization peak is prolonged close to the melting transition of a second polymorph at 111 °C; no weight loss was observed by TG/DTA at given temperature range.
[a] The glass transition temperatures are taken as half ΔCp extrapolated.
[b] Decomposition temperatures determined from onset at 5 wt% mass loss.
[c] Δwt% observed on isothermal step.
[d] Two broad overlapping endothermic transitions followed by weak exothermic transition.
[e] Overlapping transitions in order of endo-exo-endo; no weight loss was observed by TG/DTA at given temperature range.
[f] Subsequent melting-crystallization transitions.

3.3. Differential scanning calorimetry studies

Differential scanning calorimetry (DSC) studies were done to determine the transition temperatures of the dendrimers with heating and cooling rates of 10 °C/min. DSC curves of the dendrimers are illustrated in Figs. 2–4, and results from DSC measurements are summarized in Table 1. The weight of each sample was measured after the last DSC scan, and the weight losses of 0.06–1.2 wt% due to removal of water/solvent correlate with the mass losses observed in isothermal steps that was implemented in TGA measurements.

The DSC curves of the hydroxyl terminated G1 dendrimers **2** and **6** are shown in Fig. 2. In the initial heating scan compound **2** shows only melting transition (T_m) to isotropic liquid at 71.1 °C. However during the cooling scan, compound **2** shows weak exothermic peak at 31.4 °C before entering to a glassy state at about 8 °C. Furthermore, during the second heating scan T_g is observed again at 7.6 °C

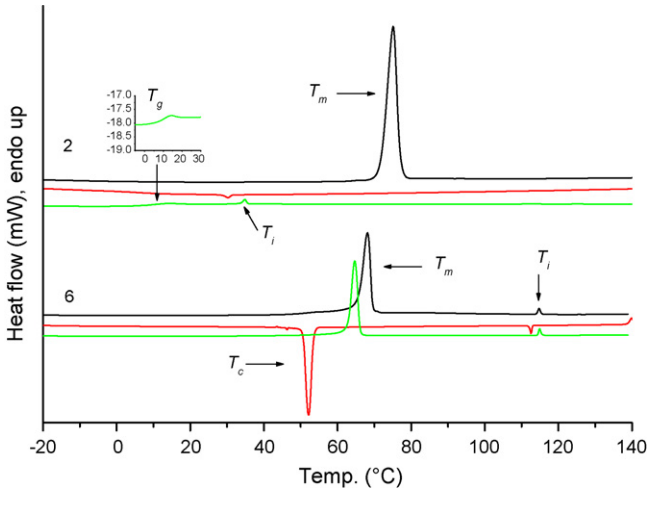

Fig. 2. DSC curves of the OH terminated G1 dendrimers. Black: first heating, red: cooling, and green: second heating. To enhance visibility of e.g. glass transitions, the *y*-axis scales are different for each compound (similarly in Figs. 3 and 4) **2** and **6**. (For interpretation of the references to color in this figure legend, the reader is referred to the web version of the article.)

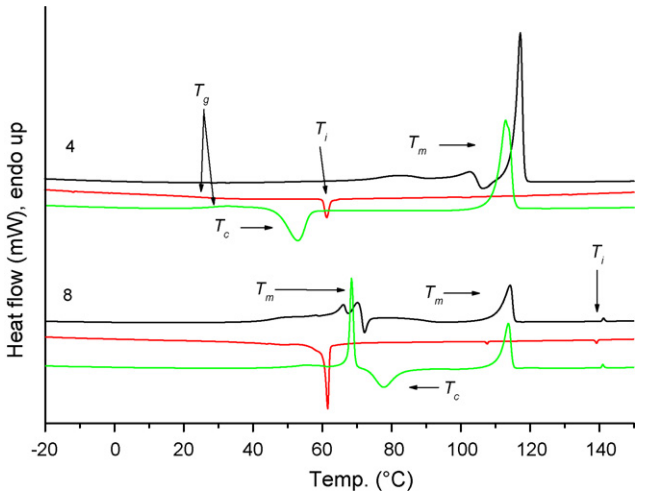

Fig. 3. DSC curves of the OH terminated G2 dendrimers. Black: first heating, red: cooling, and green: second heating. (For interpretation of the references to color in this figure legend, the reader is referred to the web version of the article.)

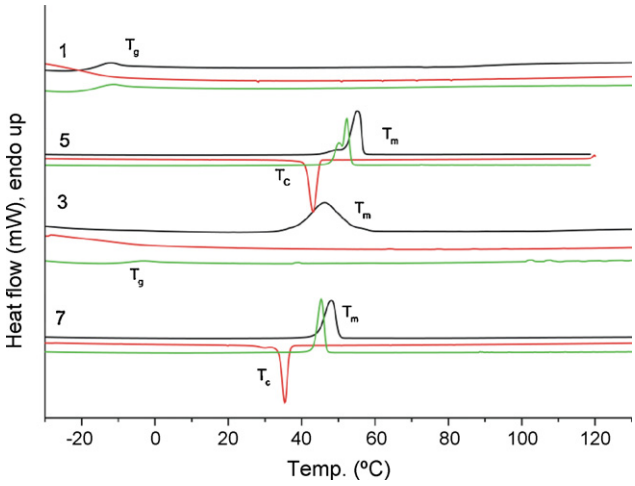

Fig. 4. DSC curves of the acetonide protected G1 and G2 dendrimers. Black: first heating, red: cooling, and green: second heating. (For interpretation of the references to color in this figure legend, the reader is referred to the web version of the article.)

but instead of entering to isotropic state dendrimer turns to LC phase (confirmed by POM), as sharp endothermic indicating clearing point is observed again at ~33.7 °C. It is rather unusual that glass transition is followed by LC phase but few examples can be found in the literature for example on monodendritic crown ethers [48,49].

The initial heating scan of compound **6** exhibit melting transition at 65.6 °C, and weak endothermic peak at 114.1 °C signifying isotropisation temperature (T_i). During the cooling scan two exothermic peaks were observed—weak peak at 113.1 °C indicating the transition from isotropic liquid phase to LC phase, followed by crystallization transition (T_c) at 53.5 °C to a solid state. Reversible thermal behavior is shown during the second heating scan, as transitions to LC phase and isotropic liquid were observed again.

The hydroxyl terminated G2 dendrimers **4** and **8** exhibited more complex thermal behavior in the DSC measurements (Fig. 3). In the initial heating scan compound **4** shows two broad overlapping endothermic transitions starting at 72.9 °C, followed by a weak exothermic transition at 104.9 °C, and finally, melting transition at 115.0 °C. These endotherms are apparently from the melting and crystallization events of different polymorph. In the cooling sequence, compound exhibit exothermic peak at 62.5 °C above glass transition. The second heating scan shows the glass transition, followed by broad exothermic peak at 46.8 °C indicating rearrangement into a crystalline phase (cold crystallization), and subsequent melting transition to isotropic liquid at 109.7 °C. Additional scans revealed that exothermic transition at around 62 °C on cooling, regardless of cooling rate, was reproducible indicating monotropic liquid crystal forming behavior. On the subsequent heating scans LC phase is absent due to cold crystallization occurring on a same temperature range.

In the case of compound **8**, initial heating scan shows overlapping sequence of endothermic and exothermic transitions indicating melting-crystallizing behavior, followed by phase transition to LC phase at 110.3 °C, and clearing point at 140.6 °C. In the cooling scan, two peaks were observed—transition from isotropic liquid to LC phase, and subsequent crystallization at 62.3 °C. During the second heating, two melting transition were found indicating the presence of polymorphism. The first melting transition at 67.4 °C was followed by exothermic peak at 73.0 °C representing rearrangement to another crystalline phase (polymorph). Subsequent phase transitions – T_m at 111.0 °C and T_i at 140.2 °C – are consistent with the first heating scan. Additional cooling-heating runs were recorded for compound **8**, in order to confirm phase transitions. As seen in Table 1, the additional runs correlate well with the previous runs, signifying thermally controllable phase transition behavior.

Melting transitions of the hydroxyl terminated G2 dendrimers, **4** and **8**, were about 45 °C higher than those of the corresponding G1 dendrimers **2** and **6**. An increase of about 25 °C was observed in isotropisation temperature of compound **8** in relative to compound **6**. In addition, since enthalpy changes (ΔH) of the compounds exhibiting transitions from LC phase to isotropic liquid (compounds **2**, **6** and **8**) were about 0.8, 2.4, 1.8 kJ mol^{-1}, respectively, it leads to a conclusion that the LC phases could be nematic.

Thermal behavior of acetonide terminated dendrimers were also studies (Fig. 4). During the first heating scans, endothermic peaks corresponding to melting transition were observed for all the protected dendrimers, except for **1**, for which only T_g at −17.8 °C was found. In the cooling run, T_cs were observed for C_{16} dendrimers **5** and **7**. In the subsequent second heating run of dendrimers **5** and **7**, corresponding melting transition were found again. In the case of C_6 dendrimers **1** and **3**, glass transitions were the only detectable phase transitions in the subsequent cooling and heating runs.

All the C_6 alkylated dendrimers exhibited glass transitions in the second heating run. The glass transition temperatures of the C_6 dendrimers increased with additional generation. In addition, hydroxyl terminated C_6 dendrimers showed higher T_g values than the corresponding acetonide protected dendrimers. The result is in good agreement with the previous studies of polyester dendrimers [37] and polyether dendrimers [33], demonstrating that increasing polarity of the end groups as well as branching increases glass transition temperature. However, none of the C_{16} dendrimers showed T_g at the temperature range of the measurements, but distinct melting transitions due to the crystalline feature of the long alkyl chain. The result is comparable with the study of Ihre et al. who reported the impact of the linear hydrocarbon chain ends on the crystallization of the otherwise amorphous polyester dendrimers [34].

3.4. X-ray powder diffraction studies

Since the hydroxyl terminated dendrimers (**2**, **4**, **6**, and **8**) showed phase transitions in DSC measurements, their crystallinity was also evaluated by X-ray powder diffraction studies at room temperature. The results are illustrated in Fig. 5. Even though the DSC measurements show apparent melting transitions for all the hydroxyl terminated dendrimers, the first generation C_6 dendrimer **2** was the only compound having diffraction pattern of sharp peaks, and thus, can be considered to be crystalline. However in the case

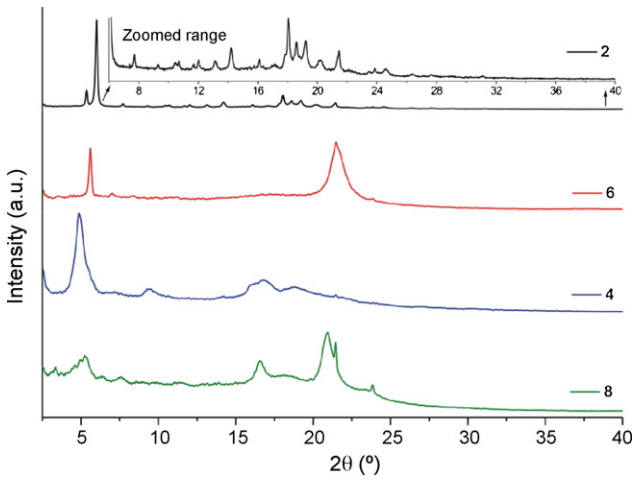

Fig. 5. X-ray powder diffraction patterns of OH terminated dendrimers **2**, **4**, **6** and **8**.

of compounds **4**, **6**, and **8**, diffraction patterns show only a few broad but intensive peaks. On the basis of the diffraction patterns and sharp melting transitions in the DSC measurements, it seems probable that the at least dendrimers **4** and **6** may assemble into two-dimensional (layered) structures.

4. Conclusions

Janus-type polyester dendrimers up to the second generation were synthesized in high yields and their thermal behavior was evaluated. Phase transitions of both acetonide and hydroxyl terminated dendrimers were determined with DSC measurements. All the compounds, except **1**, had melting transition during the first heating. All the C_{16} dendrimers (**5**–**8**) displayed both crystallization and melting transitions on subsequent cooling-heating scans, providing higher crystalline character over the dendrimers of the C_6 series. Both hydroxyl terminated C_{16} dendrimers (**4** and **8**) exhibited enantiotropic LC phases in subsequent heating-cooling-heating scans. Upon first heating, dendrimers **2** and **6** of the C_6 series exhibited only melting transitions, while on subsequent cooling both compounds showed LC phases below their melting transitions. In case of the dendrimer **2** the LC phase was reversible, thus obtained on both heating and cooling scans, while compound **6** exhibits mesomorphic transition only on cooling. Both melting and isotropisation temperatures increased along with an increase hydroxyl groups introduced by the second generation. The decomposition temperatures varied between 241 and 308 °C. The C_6 dendrimers had somewhat higher thermal stability over the corresponding C_{16} dendrimers. In case of the C_6 alkylated dendrimers, additional generation slightly increased their thermal stability. In addition, inside this group OH terminated dendrimers displayed slightly higher decomposition temperatures over the corresponding acetonide terminated ones. This is assumed to stem from hydrogen bonding interactions. Similar behavior was not observed for the C_{16} alkylated dendrimers, as all the compounds started to decompose at about the same temperature.

Acknowledgements

We thank Mr. Reijo Kauppinen for his help in running the NMR spectra, Ms. Mirja Lahtiperä for her assistance with the ESI TOF-MS spectra, and Ms. Elina Hautakangas for the elemental analysis data.

References

[1] G.R. Newkome, C.N. Moorefield, F. Vögtle, Dendrimers and Dendrons: Concepts, Syntheses and Applications, Wiley-VCH, Weinheim, 2001.
[2] J.M.J. Fréchet, D.A. Tomalia (Eds.), Dendrimers and Other Dendritic Polymers, Wiley, Chichester, 2001.
[3] S. Nummelin, M. Skrifvars, K. Rissanen, Top. Curr. Chem. 210 (2000) 1–67.
[4] E. Buchleier, W. Wehner, F. Vögtle, Synthesis (1978) 155–158.
[5] D.A. Tomalia, H. Baker, J. Dewald, M. Hall, G. Kallos, S. Martin, J. Roech, J. Ryder, P. Smith, Polym. J. 17 (1985) 117–132.
[6] G.R. Newkome, Z. Zao, G.R. Baker, V.K. Gupta, J. Org. Chem. 50 (1985) 2003–2004.
[7] C.J. Hawker, J.M.J. Fréchet, J. Am. Chem. Soc. 112 (1990) 7638–7647.
[8] T.M. Miller, T.X. Neenan, Chem. Mater. 2 (1990) 346–349.
[9] U. Boas, P.M.H. Heegaard, Chem. Soc. Rev. 33 (2004) 43–63.
[10] E.R. Gillies, J.M.J. Fréchet, Drug Deliv. Today 10 (2005) 35–43.
[11] A. Adronov, J.M.J. Fréchet, Chem. Commun. (2000) 1701–1710.
[12] V. Balzani, P. Ceroni, M. Maestri, V. Vicinelli, Curr. Opin. Chem. Biol. 7 (2003) 657–665.
[13] M.-S. Choi, T. Yamazaki, I. Yamazaki, T. Aida, Angew. Chem. Int. Ed. 43 (2004) 150–158.
[14] R. van Heerbeek, P.C.J. Kamer, P.W.N.M. van Leeuwen, J.N.H. Reek, Chem. Rev. 103 (2002) 3717–3756.
[15] C. Liang, J.M.J. Fréchet, Prog. Polym. Sci. 30 (2005) 385–402.
[16] D. Méry, D. Astruc, Coord. Chem. Rev. 250 (2006) 1965–1979.
[17] A.-M. Caminade, P. Servin, R. Laurent, J.-P. Majoral, Chem. Soc. Rev. 37 (2008) 56–67.
[18] C.J. Hawker, K.L. Wooley, J.M.J. Fréchet, J. Chem. Soc. Perkin Trans. 1 (1993) 1287–1297.
[19] E.R. Gillies, J.M.J. Fréchet, J. Am. Chem. Soc. 124 (2002) 14137–14146.
[20] J. Ropponen, S. Nummelin, K. Rissanen, Org. Lett. 6 (2004) 2495–2497.
[21] V. Percec, M.R. Imam, T.K. Bera, V.S.K. Balagurusamy, M. Peterca, P.A. Heiney, Angew. Chem. Int. Ed. 44 (2005) 4739–4745.
[22] P. Wu, M. Malkoch, J.N. Hunt, R. Vestberg, E. Kaltgrad, M.G. Finn, V.V. Fokin, K.B. Sharpless, C.J. Hawker, Chem. Commun. (2005) 5775–5777.
[23] N.R. Luman, M.W. Grinstaff, Org. Lett. 7 (2005) 4863–4866.
[24] M. Yang, W. Wang, F. Yuan, X. Zhang, J. Li, F. Liang, B. He, B. Minch, G. Wegner, J. Am. Chem. Soc. 127 (2005) 15107–15111.
[25] I. Bury, B. Heinrich, C. Bourgogne, D. Guillon, B. Donnio, Chem. Eur. J. 12 (2006) 8396–8413.
[26] O. Lukin, V. Gramlich, R. Kandre, I. Zhun, T. Felder, C.A. Schalley, G. Dolgonos, J. Am. Chem. Soc. 128 (2006) 8964–8974.
[27] T. Tuuttila, J. Lipsonen, M. Lahtinen, J. Huuskonen, K. Rissanen, Tetrahedron 64 (2008) 10590–10597.
[28] I.M. Saez, J.W. Goodby, Chem. Eur. J. 9 (2003) 4869–4877.
[29] I. Bury, B. Donnio, J.-L. Gallani, D. Guillon, Langmuir 23 (2007) 619–625.
[30] J. Lenoble, S. Campidelli, N. Maringa, B. Donnio, D. Guillon, N. Yevlampieva, R. Deschenaux, J. Am. Chem. Soc. 129 (2007) 9941–9952.
[31] C. Lee, E.R. Gillies, M.E. Fox, S.J. Guillaudeu, J.M.J. Fréchet, E.E. Dy, F.C. Szoka, Prog. Natl. Acad. Sci. U.S.A. 103 (2006) 16649–16654.
[32] E.G. Gillies, E. Dy, J.M.J. Fréchet, F.C. Szoka, Mol. Pharmaceut. 2 (2005) 129–138.
[33] K.L. Wooley, C.J. Hawker, J.M. Pochan, J.M.J. Fréchet, Macromolecules 26 (1993) 1514–1519.
[34] H. Ihre, A. Hult, J.M.J. Fréchet, I. Gitsov, Macromolecules 31 (1998) 4061–4068.
[35] C.-O. Turrin, V. Maraval, J. Leclaire, E. Dantras, C. Lacabanne, A.-M. Caminade, J.-P. Majoral, Tetrahedron 59 (2003) 3965–3973.
[36] J. Ropponen, J. Tamminen, M. Lahtinen, J. Linnanto, K. Rissanen, E. Kolehmainen, Eur. J. Org. Chem. (2005) 73–84.
[37] J. Ropponen, T. Tuuttila, M. Lahtinen, S. Nummelin, K. Rissanen, J. Polym. Sci: Part A: Polym. Chem. 42 (2004) 5574–5586.
[38] O. Ozturk, T.J. Black, K. Perrine, K. Pizzolato, C.T. Williams, F.W. Parsons, J.S. Ratliff, J. Gao, C.J. Murphy, H. Xie, H.J. Ploehn, D.A. Chen, Langmuir 21 (2005) 3998–4006.
[39] V. Percec, A.E. Dulcey, V.S.K. Balagurusamy, Y. Miura, J. Smidrkal, M. Peterca, S. Nummelin, U. Edlund, S.D. Hudson, P.A. Heiney, H. Duan, S.N. Magonov, S.A. Vinogradov, Nature 430 (2004) 764–768.
[40] V. Percec, M.N. Holerca, S. Nummelin, J.J. Morrison, M. Glodde, J. Smidrkal, M. Peterca, B.M. Rosen, S. Uchida, V.S.K. Balagurusamy, M.J. Sienkowska, P.A. Heiney, Chem. Eur. J. 12 (2006) 6216–6241.
[41] V. Percec, M. Peterca, M.J. Sienkowska, M.A. Ilies, E. Aqad, J. Smidrkal, P.A. Heiney, J. Am. Chem. Soc. 128 (2006) 3324–3334.
[42] V. Percec, J. Smidrkal, M. Peterca, C.M. Mitchell, S. Nummelin, A.E. Dulcey, M.J. Sienkowska, P.A. Heiney, Chem. Eur. J. 13 (2007) 3989–4007.
[43] V. Percec, B.C. Won, M. Peterca, P.A. Heiney, J. Am. Chem. Soc. 129 (2007) 11265–11278.
[44] V. Percec, M. Peterca, A.E. Dulcey, M.R. Imam, S. D: Hudson, S. Nummelin, P. Adelman, P.A. Heiney, J. Am. Chem. Soc. 130 (2008) 13079–13094.
[45] M. Malkoch, E. Malmström, A. Hult, Macromolecules 35 (2002) 8307–8314.
[46] V. Percec, C.-H. Ahn, T.K. Bera, G. Ungar, D.P.J. Yeardley, Chem. Eur. J. 5 (1999) 1070–1083.
[47] J.S. Moore, S.I. Stupp, Macromolecules 23 (1990) 65–70.
[48] V. Percec, W.-D. Cho, G. Ungar, D.J.P. Yeardley, Chem. Eur. J. 8 (2002) 2011–2025.
[49] F. Ammar-Khodja, S. Guermouche, M.-H. Guermouche, P. Judenstein, J.-P. Bayle, Chromatographia 70 (2009) 497–502.